Relationship between the Northern Hemisphere Joule heating and geomagnetic activity in the southern polar cap

P. Ballatore, L. J. Lanzerotti, G. Lu, D.J. Knipp

JOURNAL OF GEOPHYSICAL RESEARCH, VOL. 105, NO. A12, PAGES 27,167–27,177, DECEMBER 1, 2000

Relationship between the Northern Hemisphere Joule heating and geomagnetic activity in the southern polar cap

P. Ballatore

Laboratoire de Physique et Chimie de l'Environnement/CNRS, 45071 Orleans, France

L. J. Lanzerotti

Bell Laboratories, Lucent Technologies, Murray Hill, NJ 07974, USA

G. Lu

NCAR, UCAR, Boulder, CO 80307, USA

D. J. Knipp

Department of Physics, U.S. Air Force Academy, Colorado Springs, CO 80840, USA

Abstract. One of the most important effects from the coupling of the solar wind to the magnetosphere-ionosphere system is the Joule heating (JH) of the atmosphere that is produced by the energy dissipation of ionospheric currents and geomagnetic field-aligned precipitating particles. At present, the most commonly used technique to estimate the global JH rate is the Assimilative Mapping of Ionospheric Electrodynamics (AMIE) procedure. Here we describe a study of the relationship of the Northern Hemisphere JH and the Southern Hemisphere polar geomagnetic index AES-80 during a magnetic storm on October 18-23, 1995 (when both quantities are available). The purpose is to study the effects of the Northern-Southern Hemispherical asymmetry on the correlation between JH and geomagnetic indices. Our results confirm a higher contribution to JH from regions associated with eastward currents. Moreover, we find that the best correspondence between the northern JH and the AES-80 occurs during negative interplanetary magnetic field (IMF) B_z and B_y conditions. We discuss how this result is in agreement with the magnetospheric-ionospheric model that considers, during negative IMF B_z and B_y, an increase of conductance in the regions associated with eastward currents in the Northern Hemisphere. Our observations related to the best estimation of Southern Hemisphere JH are in agreement with the same model too. We also find a "saturation" effect for large values of northern JH: the JH−AES-80 correlation breaks down for intervals with JH > 190 gigawatt (GW), during the highest geomagnetic perturbations, and a negative IMF B_z that exceeds -20 nT. This "saturation" is in part attributed to the onset of hemispherical asymmetry due to the solar wind pressure with respect to the Earth-dipole orientation under severe storm conditions.

1. Introduction

One of the more important effects that arises from the coupling of the solar wind with the magnetosphere-ionosphere system is the atmospheric Joule heating (JH) that is produced by the dissipation of ionospheric currents and geomagnetic field-aligned precipitating particles [e.g., *Akasofu,* 1981]. Presently, the technique most commonly used for estimating the global JH rate is the Assimilative Mapping of Ionospheric Electrodynamics (AMIE) procedure [*Richmond and Kamide,* 1988].

The calculation of the global JH rate is complex and requires the use of simultaneous ground-based multi-instrument data and satellite observations. Because of this complexity, the possibility of using one or more geomagnetic indexes as a proxy for the JH rate has been considered in the past. Examinations of the correlations of calculated JH rates with the cross-polar-cap

Paper number 1999JA000390.
0148-0227/00/1999JA000390$09.00

potential, the *AE* index, or the polar cap (PC) index suggested that each might be a reasonable proxy for the JH rate [*Chun et al.,* 1999, and references therein].

Because of the significantly sparser data availability for the Southern Hemisphere than for the north, previous calculations of the JH rate have been carried out mainly for the Northern Hemisphere; comparisons between the JH and other geomagnetic parameters have been made using only Northern Hemisphere geomagnetic indices. Although rather good magnetospheric conjugacy is expected between the Northern and Southern Hemispheres, north-south asymmetries have also been observed, mostly related to different local seasonal ionospheric conductivities [e.g., *Mizera et al.,* 1987; *Newell and Meng,* 1988; *Maclennan et al.,* 1991].

Recently, a new geomagnetic index, AES-80, has been calculated and studied for southern polar geomagnetic activity. This index was derived to take advantage of the increasing amount of data from high-latitude Automatic Geophysical Observatories (AGOs) in the Antarctic [*Rosenberg and Doolittle,* 1992]. In particular, in its present embodiment the determination of the AES-80 index uses multistation geomagnetic data from Antarctic stations spaced at about -80°corrected geomagnetic (CGM) latitude [*Ballatore et al.,* 1998a]. Similar to other *AE*-like indices [e.g., *Saroso et al.,* 1992], AES-80 indicates the global geomagnetic disturbances (and associated ionospheric currents) above the region considered [*Ballatore et al.,* 1998a, 1998b; *Ballatore and Maclennan,* 1999]. AES-80 covers a wider geomagnetic range near the southern polar cap than does the single station-determined polar cap index (e.g., described by *Troshichev et al.,* [1988]).

In this paper we compare the Northern Hemisphere integrated JH rate with the geomagnetic activity at high southern latitudes as represented by the AES-80 parameter for a large magnetic storm in 1995, when both parameters, the JH integrated in the northern hemisphere (JH(N)) and AES-80, were available. In the context of previous results that demonstrated good correspondence between the northern JH rate and geomagnetic activity in the northern polar cap (including the use of the northern polar cap index [*Chun et al.,* 1999]), the present study was implemented as an investigation of north-south asymmetry.

In the following we consider only the AES-80 index as the indicator of southern high-latitude geomagnetic activity because, during the large storm period under investigation, it is the only Southern Hemisphere index available. In fact, at present the PC index from Vostok is not available for the year 1995.

2. Experimental Observations and Data Analysis

Both the JH(N) rate and the AES-80 data were available for the magnetic storm event of October 18-23, 1995. The JH(N) rate data were derived, at 5-min resolution, using the AMIE procedure [*Richmond et al.,* 1990]. Possible limitations of the AMIE estimation of JH(N) have been previously identified. These include effects of neutral winds [*Cooper et al.,* 1995; *Lu et al.,* 1995] and/or unaccounted-for small-scale variations in the electric field [*Codrescu et al.,* 1995]. Moreover, if smaller grid scale sizes are used in the AMIE computation, the obtained JH can be as much as a factor of 2 larger than the rate given by the standard computation [*Li et al.,* 1998]. Therefore it is not excluded that, at times, the real physical JH rate could be larger than the values used here.

The AES-80 polar index is derived according to a standard procedure [*Ballatore et al.,* 1998a] using geomagnetic data from the four Antarctic stations illustrated in Figure 1. With respect to the AES-80 index used in previous studies, the index used herein does not include data from the station AGO P1, as they were not available for the period considered. However, P1 is relatively close to P4, and the four stations illustrated in Figure 1 are sufficiently regularly spaced in longitude that this four-station AES-80 can be considered a good approximation of AES-80 in the southern polar geomagnetic region. This index (and its components ALS-80 and AUS-80) have been derived at 1-min resolution, and their median values over intervals of 5-min have been calculated for comparison with the 5-min-resolution JH(N) data.

Increasing from the lowest panel, Figure 2 contains plots as a function of UT of the southern polar indexes ALS-80, AUS-80, and AES-80 and the JH(N) and JH(S) (this is the best estimation of the JH integrated in

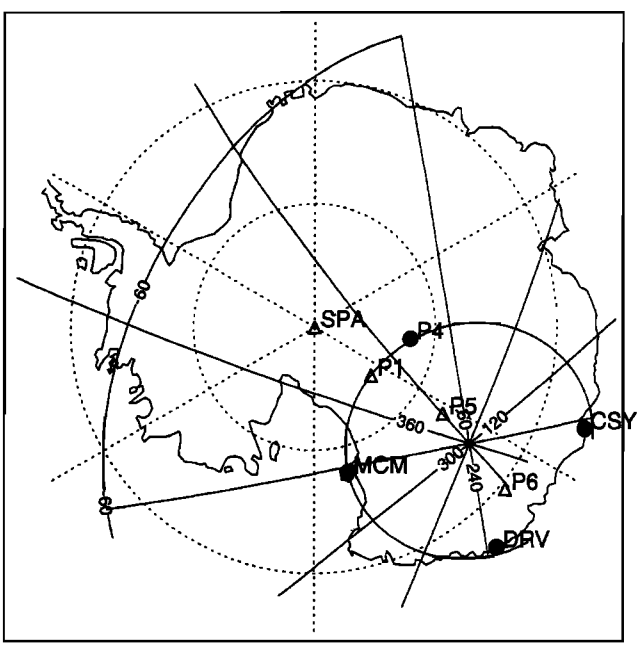

Figure 1. Stations used for the computation of AES-80.

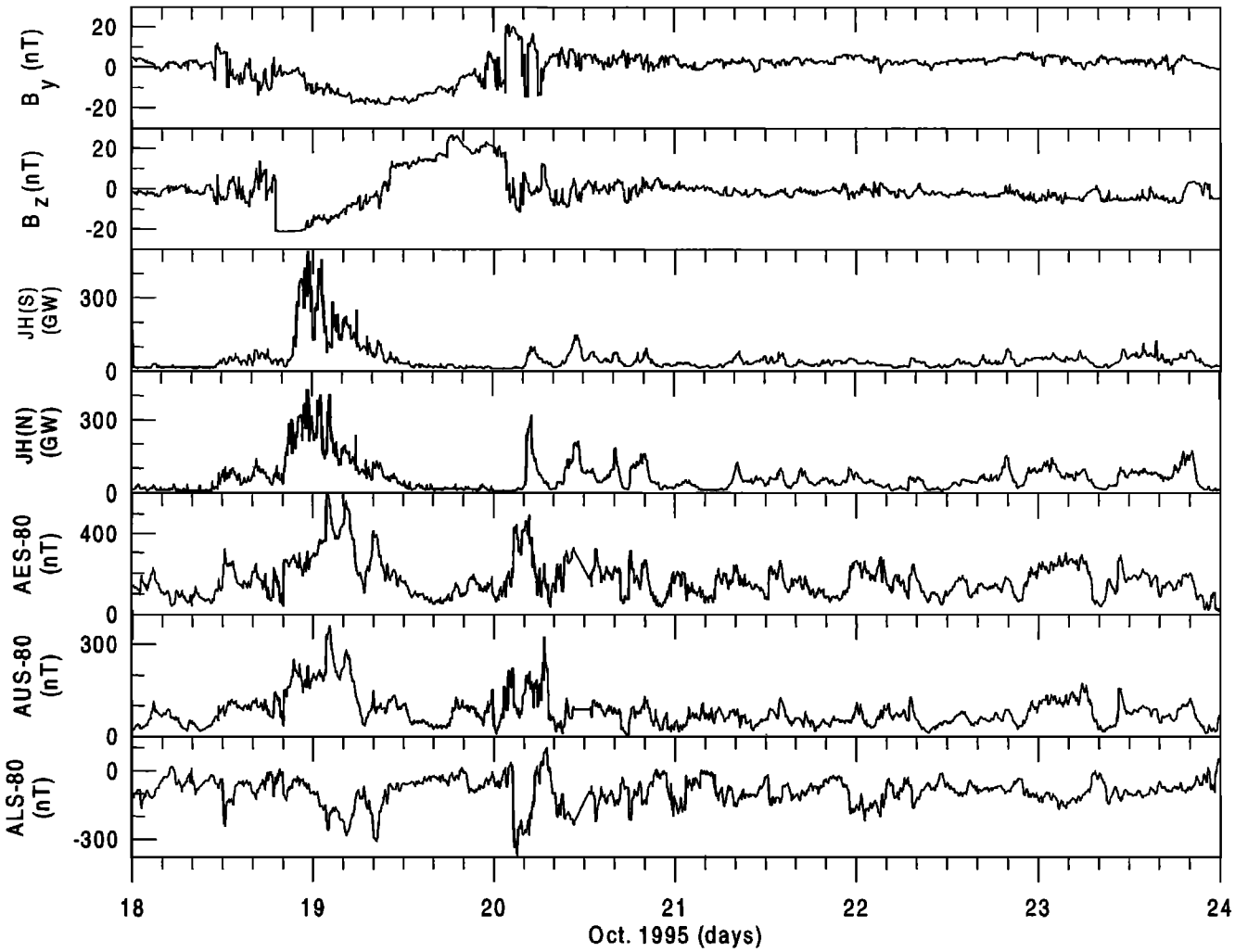

Figure 2. From the top to the bottom the panels show IMF B_y, IMF B_z, JH(N) rate, JH(S) rate, AES-80, ALS-80, and AUS-80 for the period from October 18 until October 23 1995.

the Southern Hemisphere) rates. The upper two panels plot the two interplanetary magnetic field (IMF) components B_z and B_y (retrieved from the WWW site of the Wind satellite database). The passage of an interplanetary magnetic cloud (ICME) during the last portion of October 18 and on October 19 is very evident in the variation of the IMF B_z component.

Visually, the intensity-time plots in Figure 2 show rather good correspondences between variations of AES-80 and the JH(N) rate under conditions of large IMF B_y and B_z (e.g., during day 19) and when IMF B_y and B_z are smaller. There are also a few occasions of high AES-80 during small JH(N). Such cases might be instances of underestimation of JH(N) or instances of hemispherical asymmetry of Joule heating.

In order to quantify the comparison between the JH(N) and the AES-80 we have calculated correlation coefficients using the data at 5-min resolution. The correlation coefficients are reported in the first column of Table 1. We find rather good correlations with the JH(N) for AES-80 and AUS-80. Similar correlations were calculated after averaging the JH(N) and the polar indexes over longer time intervals. These correlation coefficients are also shown in Table 1. An increase in the values of the correlation coefficients is found for the longer averages. The confidence levels for the correlation coefficients shown in Table 1 are all higher than 99.9% for AES-80 and AUS-80; the confidence level is only ~95% for ALS-80 when time intervals of 3 hours or longer are considered.

Considering the best fits given by the correlations of JH(N) with AES-80 and AUS-80 on a 12-hour timescale (coefficients 0.81 and 0.89, respectively; Table 1) we determined estimated proxy values for JH(N), JH(N)*, from the southern index (AES-80). In Figure 3 we show the scatterplots for the JH(N)* versus JH(N). The data points have a rather small scatter around the line JH(N)*=JH(N) (indicated by the solid line). Similar JH(N)* estimates were previously calculated by *Chun et al.* [1999] using geomagnetic indices calculated in the Northern Hemisphere. The correlation coefficients that we show in Figure 3, although good, are slightly smaller

Table 1. Correlation Coefficients of AES-80, ALS-80, and AUS-80 With JH(N) for Various Averaging Intervals[a]

	Time Resolution				
	5-min n=1693	1-hour n=144	3-hour n=48	6-hour n=24	12-hour n=12
AES-80	0.64	0.69	0.75	0.76	0.81
ALS-80	0.34	0.38	0.47	0.47	0.57
AUS-80	0.71	0.75	0.80	0.87	0.89

[a]Here n indicates the number of data points used in each correlation.

than similar ones obtained by *Chun et al.* [1999] for the Northern Hemisphere.

In order to study the JH(N)−AES-80 relationship under different disturbance conditions of the geomagnetic field, we redetermined the correlations reported in the left-hand column of Table 1 for different orientations of the interplanetary magnetic field (IMF). The results are shown in Figure 4a for AES-80 versus JH(N), in Figure 4b for ALS-80 versus JH(N), and in Figure 4c for AUS-80 versus JH(N) for IMF $B_z < 0$ and IMF $B_z > 0$ and for the two cases of IMF $B_y < 0$ and IMF $B_y > 0$. The 12 correlations are all significant at a confidence level above 99.9%. Smaller correlations are again obtained for the ALS-80−JH(N) investigation. The IMF direction that gives the best correlation is for B_z and B_y both negative. The correlation coefficients that are shown in these cases have been calculated using only data for JH(N) < 190 gigawatt (GW). Above about this value, no clear correlation exists.

The same correlations as examined in Figure 4 were also calculated including a delay (5-min to 1-hour) between the interplanetary values and the ground-based data. No significant differences were found.

In order to examine further the apparent "saturation" effect for JH > 190 GW that was obtained for the correlations with the negative IMF B_y and B_z values, we have plotted in Figure 5 the histograms of the distributions of IMF B_y and B_z values (bottom and middle panels) and of the modulus B_T of the vector sum of B_z and B_y (top panel). We note that B_T has values > 15 nT only for JH(N) > 190 GW and that the distribution of B_z is clearly shifted to larger negative numbers for JH(N) > 190 GW than for JH < 190 GW. These characteristics are also evident when a delay (delays of 1/2 hour and 1 hour were considered) is introduced between the interplanetary and the ground-based data.

Next, the estimates of JH(N)* from AES-80 and AUS-80 were calculated using only data with negative IMF B_y and B_z and JH(N) < 190 GW. The results are illustrated in Figure 6 for data averaged over 12-hour intervals. Comparing Figure 3 with Figure 6, we see that the correlations are larger in the latter case, with the slopes of the linear correlation lines all close to one.

3. Discussion

Previous studies using the AES-80 index demonstrated a significant correlation of this parameter with other planetary geomagnetic indexes, including Northern Hemisphere indices [*Ballatore et al.*, 1998a, 1998b; *Ballatore and Maclennan*, 1999]. Therefore, since Northern Hemisphere geomagnetic indices are in agreement with JH rates calculated in the Northern Hemisphere [*Chun et al.*, 1999], one might expect that the AES-80 can also provide information about the JH rates, especially in the Southern Hemisphere.

The time-intensity relationships shown in Figure 2 resemble similar plots as a function of UT that were reported for JH rates and *AE* (the northern Auroral Electrojet index) by *Baumjohann and Kamide* [1984]. In that paper, *Baumjohann and Kamide* [1984] examined 3 days of data at 5-min resolution, and a correlation coefficient of 0.74 was found between *AE* and JH.

We have investigated the correlation at 5-min resolution between JH and the *AE* index calculated with the use of 61 stations, AE(61), between 55°and 76°CGM latitude (in the Northern and Southern Hemispheres, however, the addition due to the Southern Hemisphere is not very significant owing to fewer stations being there) for our period October 18-23, 1995. This latitude range should cover the maximum electrojet intensity better than the standard *AE* index, which is determined from 12 longitudinally spaced stations between 0°and 70°CGM latitude. We find a correlation

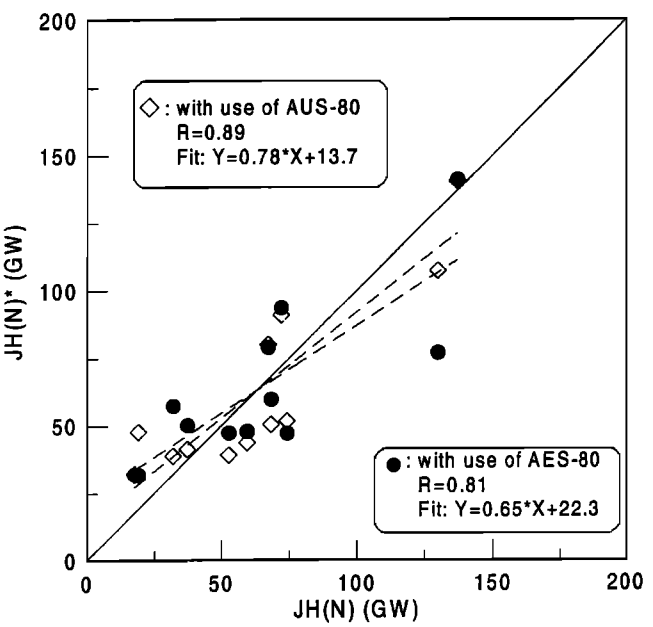

Figure 3. Scatterplot of data points (averaged over 12-hour intervals) of JH(N)* estimated using AES-80 and AUS-80 parameters versus JH(N) determined by the AMIE procedure. The dashed lines correspond to the best fits for the two groups of data. The correlation coefficients R and the equations of the fits are indicated. The solid line corresponds to the ideal case JH(N)*=JH(N).

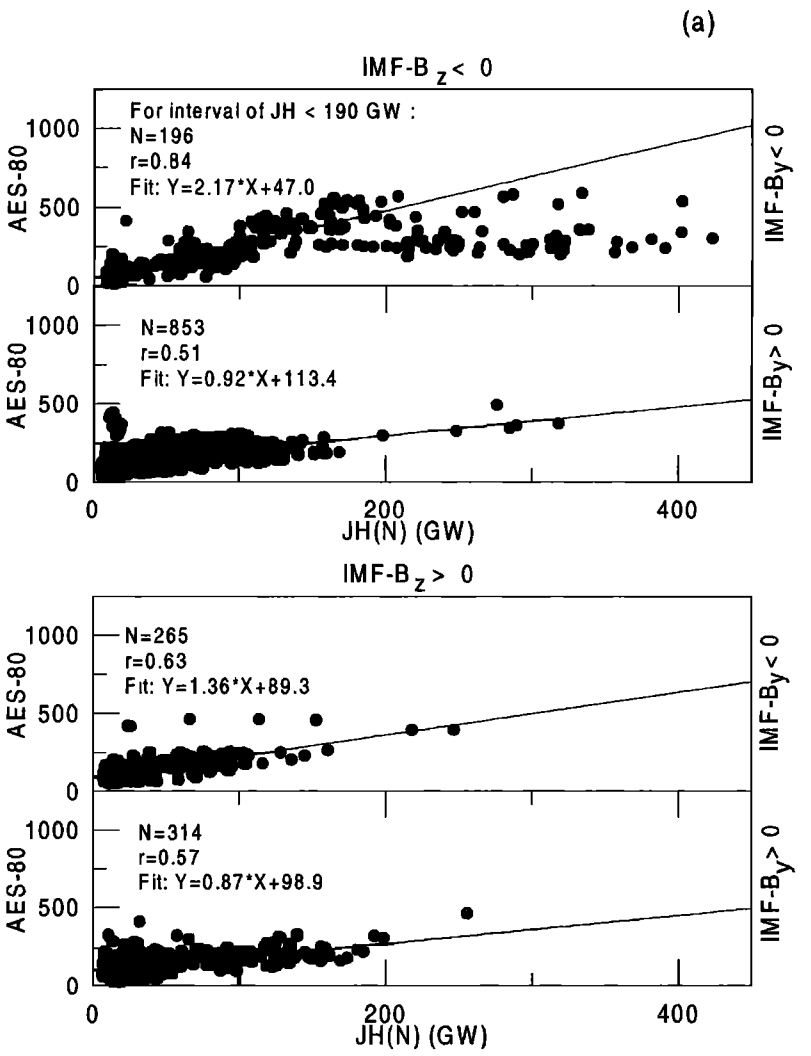

Figure 4. Scatterplots of (a) AES-80, (b) ALS-80, and (c) AUS-80 versus JH(N), separately for positive and negative IMF B_z and IMF B_y. For each panel the number of data points used, the correlation coefficient, and the best fit line equation (which is drawn as a solid line) are given.

coefficient of 0.82. The correlation coefficients of JH with AU(61) and AL(61) are found to be 0.71 and 0.74, respectively. The correlation value that is obtained for AU(61) is equal to the one obtained for AUS-80 at the same 5-min resolution (Table 1). This is a very compelling result, especially considering the fact that the compared parameters are for opposite hemispheres.

When we calculated JH(N)* from AES-80 (or AUS-80) and compared it with the measured JH(N) (Figure 3), we found significant, but lower, correlations than were found for estimates from the northern *AE* or PC indices [*Chun et al.*, 1999]. This result might be in part related to the seasonal dependence of ionospheric conductance, which can affect results obtained in opposite hemispheres.

The JH(N) rates have higher correlation with AUS-80 than with ALS-80, or even with AES-80 itself (Table 1). This could be related to a better correspondence of AUS-80 with the Northern Hemisphere with respect to ALS-80. In fact, the correlation coefficient between ALS-80 and AL(61) is 0.40 for the October 18-23 interval, and it is 0.49 between AUS-80 and AU(61). This result is rather surprising, and it has to be considered specifically in the context of the large storm period studied here. In fact, on much larger timescales it has been previously reported that the ALS-80 parameter has a higher correlation than does AUS-80 with any northern or planetary geomagnetic indices [*Ballatore et al.*, 1998a; *Ballatore and Maclennan*, 1999].

Additional geomagnetic causes could affect the fact that we find that AUS-80 correlates better with the northern JH during the magnetic storm than does either ALS-80 or AES-80. In the previously cited paper by *Baumjohann and Kamide* [1984], they also reported the correlations of AU and AL with Joule heating. However, for these two parameters (AU and AL), instead of using the global JH, *Baumjohann and Kamide* [1984] used the JH integrated over cells of only eastward currents and of only westward currents, respectively. Even given this difference, the correlation coefficient that

they obtained for AU (0.73) was still slightly higher than the value that they obtained for AL (0.67), which is consistent with our results.

We can therefore interpret our apparent contradictory result by noting that the eastward currents are localized in a region of typically lower ionospheric conductivity in comparison to westward currents [*Vickrey et al.*, 1982]. Therefore the higher electric field regions (corresponding to the eastward currents; AUS-80 in our case) are contributing relatively more to the global Joule heating.

We calculated the correlations of JH with AU(61) and AL(61) using values of AU(61) and AL(61) between 0 and |500| nT (the number of 5-min-resolution data points was 1649 and 1512 for AU(61) and AL(61), respectively). We found correlation coefficients of 0.70 and 0.58 for AU(61) and AL(61), respectively. These results confirm the expectation of a higher contribution of eastward currents to JH in comparison to the westward currents.

We find a much better agreement between AES-80 and the measured JH(N) for the cases of IMF $B_z < 0$ and $B_y < 0$ (Figure 4a). During southward IMF, negative B_y conditions are known to produce enhancements in the conductivity associated with eastward currents at northern high latitudes and enhancements in the conductivity associated with westward currents at southern high latitudes. Positive IMF B_y conditions produce just the opposite enhancements [e.g., *Friis-Christensen and Wilhjelm*, 1975; *Belehaki and Rostoker*, 1996]. Therefore a negative IMF B_y, with its correspondingly enhanced conductivity in the eastward current region in the Northern Hemisphere, will tend to reduce the higher contribution to JH(N) from seasonally dependent eastward current with respect to westward. The opposite will be true for positive B_y, and a larger hemispherical difference will occur.

We found a "saturation" effect to occur in the correlation of JH(N) with the southern high-latitude AES-80 when IMF B_z and B_y are both negative (Figure 4a):

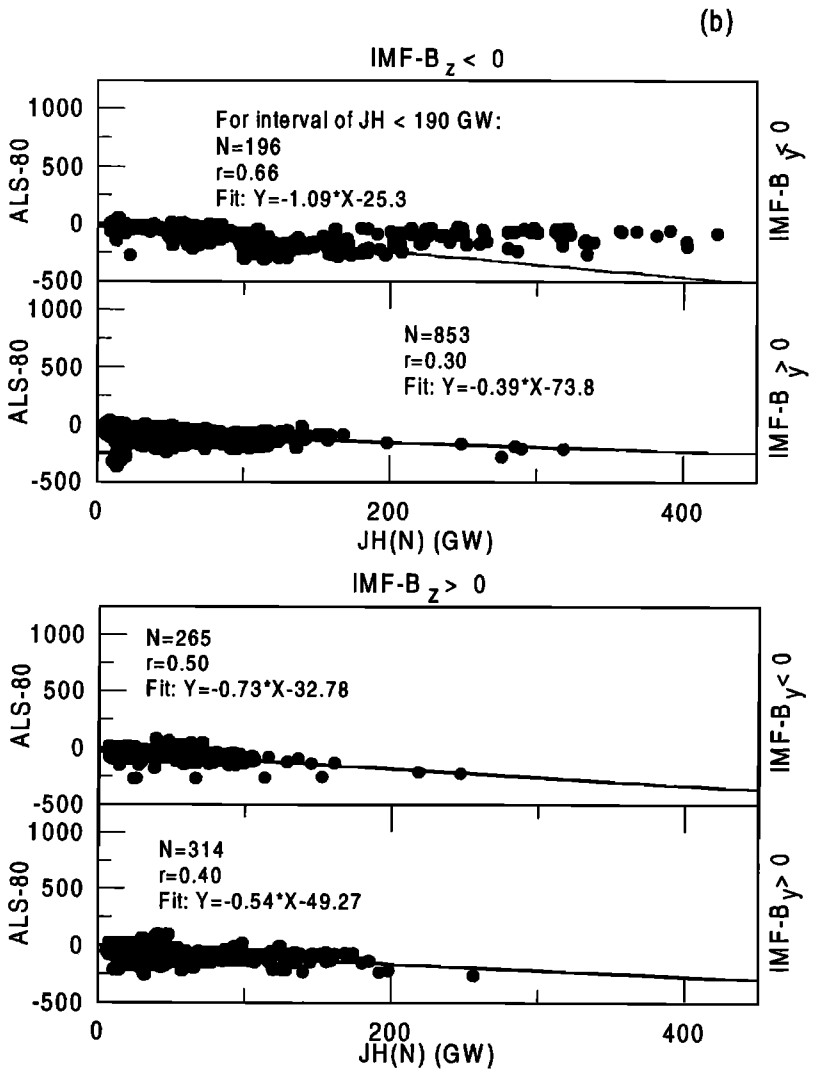

Figure 4. continued

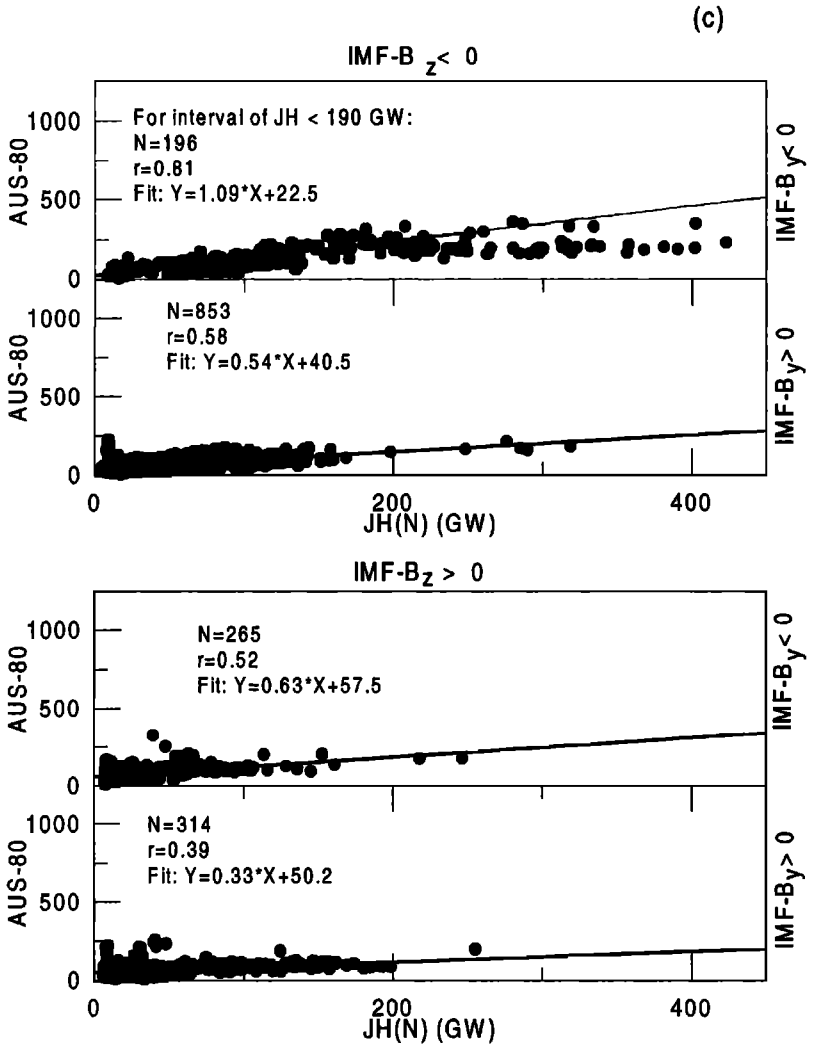

Figure 4. continued

no correlation was found between the two quantities for JH(N) > 190 GW. We also found that larger values of JH(N) occurred under conditions of larger values of negative B_z and B_T (Figure 5), where B_T is equal to $(B_z^2 + B_y^2)^{1/2}$. In contrast, an investigation (not shown here) of the distributions of other interplanetary parameters (such as the solar wind speed and proton density) showed no similar features for JH(N) larger than 190 GW.

Values of B_z and B_y that are close to zero nT correspond to the establishment of an effect of the interplanetary flow on the magnetospheric configuration which is relatively symmetric with respect to the north-south geomagnetic axis compared to the case of larger values of B_z and B_y [e.g., *Belon et al.*, 1969, and references therein]. In order to investigate how much this effect might affect our results, we computed the same correlations as in Table 1 for values of B_y and B_z in intervals of (-2, 2) nT or (-1, 1) nT. We found no statistical increase in the correlations. Also, if we include a delay between IMF and JH(N) (related to the propagation time from the satellite to the magnetosphere), no increase of correlation is found. Nevertheless, large values of B_T (> 15 nT) produce different magnetic pressures on the Northern and Southern Hemispheres such that a decrease of hemispherical conjugacy might be expected during some seasons. The open northern and southern polar caps, which are more directly associated with the interplanetary medium than other latitudes, will likely be affected differently by this north-south inclination of the IMF and of the solar wind flow. Concerning this, we mention the previous findings of *Belon et al.* [1969], who found that during disturbed periods (contrary to the quietest periods) the similarity of details of north-south auroral features, irrespective of their conjugacy, deteriorate rapidly with increasing latitude. This was attributed to the large stretching of magnetic field lines toward the magnetospheric tail and the presence of localized electric/magnetic fields in the magnetosphere [*Belon et al.*, 1969]. In particular, in a geomagnetically disturbed period during March 1968 the displacement of the auroral zone was attributed to the existence of an asymmetric distortion of geomagnetic field lines due to solar wind pression and Earth-dipole orientation, and it

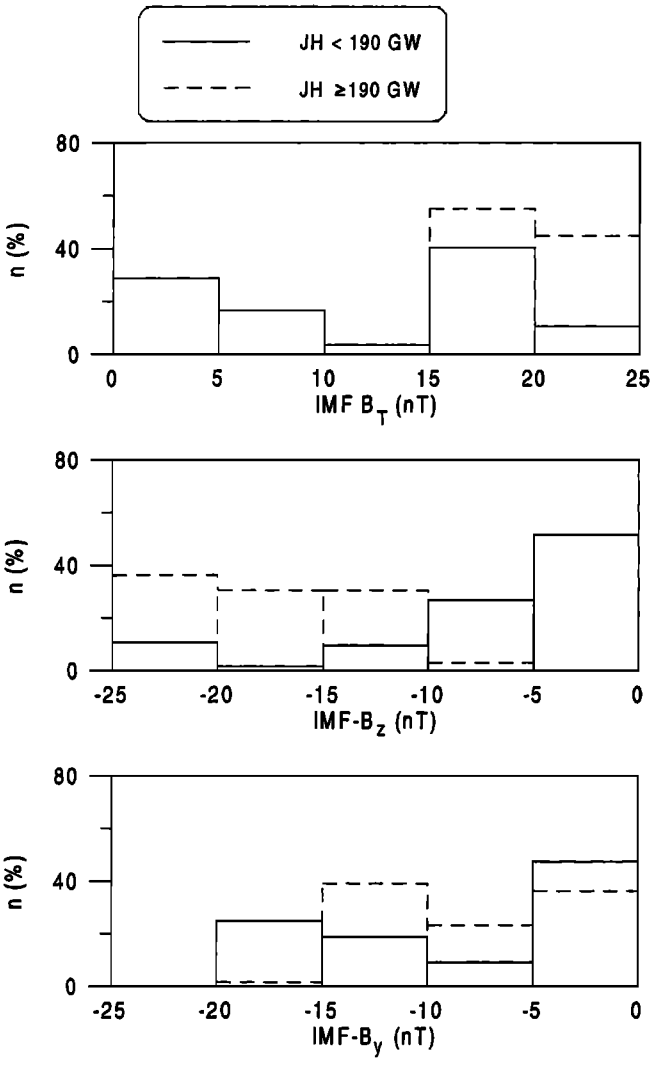

Figure 5. Histogram of the distribution of IMF B_y and B_z values and of their vectorial sum B_T for JH(N) < 190 GW (solid line) and < 190 GW (dashed line).

was found that this distortion is a very strong function of the geomagnetic activity at latitudes between 65°and 72°[*Belon et al.*, 1969, and references therein].

Furthermore, conditions of very negative B_z are associated with a high degree of merging of the IMF with the magnetosphere and therefore with the associated high increase of geomagnetic activity. Such conditions can also affect the observed decrease in the correlation for JH > 190 GW. Under conditions of high geomagnetic activity a shift of the auroral oval to lower latitudes is expected [*Kamide et al.*, 1976]. Therefore the polar cap (and its related AES-80 index) will be located farther from the source of major JH in comparison to the quieter periods. This will also affect the correlations.

We did show that, if we calculate the proxy-estimated JH(N), JH(N)*, from the AES-80 index for small values of JH(N) (and therefore for small values of the IMF B_z and B_y), a correlation coefficient well above 0.9 was found between the estimated and the measured JH(N) (Figure 6).

In Figure 7, histograms of occurrence of IMF B_z, AU(61), and AL(61) are shown separately for positive and negative IMF B_y conditions for the October 1995 geomagnetic storm interval. Only data occurring during intervals of JH < 190 GW are plotted. The histograms in Figure 7 show a shift of IMF B_z toward higher negative values during negative IMF B_y, which could affect, in part, our results. However, such a shift would also be associated with an increase of both eastward and westward currents for negative B_y. While the histograms of Figure 7 show a clear shift for AU(61) toward higher values, the AL(61) shift toward more negative values is very slight. This result is consistent with the expected increase of ionospheric conductivity associated with eastward currents during negative IMF B_y for the Northern Hemisphere [*Friis-Christensen and Wilhjelm*, 1975; *Belehaki and Rostoker*, 1996].

In order to verify that the results that we obtained are significantly affected by the north-south conjugacy or asymmetry of the magnetospheric system, we have considered the best estimate of the Southern-Hemisphere-integrated JH, JH(S), which is plotted in Figure 2 (third panel from the top) for the time interval considered. We have reported results of the correlations between AES-80, ALS-80, and AUS-80 with the 5-min JH(S) in Table 2 for different orientations of the IMF. We stress that this is not a quantitatively significant comparison between the southern polar cap geomagnetic activity and the JH(S), owing to lower reliability of JH(S). In fact, the data availability for the Southern Hemisphere

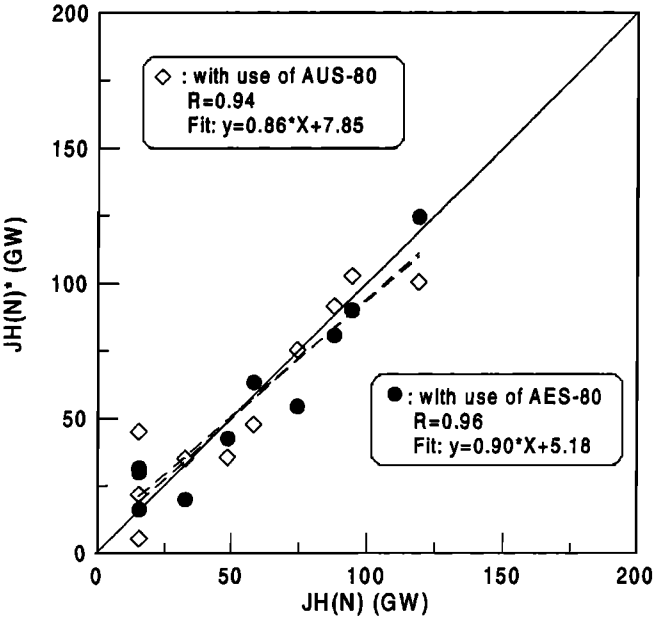

Figure 6. Scatterplot of data points (averages over 12-hour intervals) of JH(N)* estimated using AES-80 and AUS-80 parameters versus JH(N) using only data with JH(N) < 190 GW and negative IMF B_y and B_z. The dashed lines correspond to the best fits for the two groups of data. The correlation coefficients R and the equation of the fits are indicated. The solid line corresponds to the ideal case JH(N)*=JH(N).

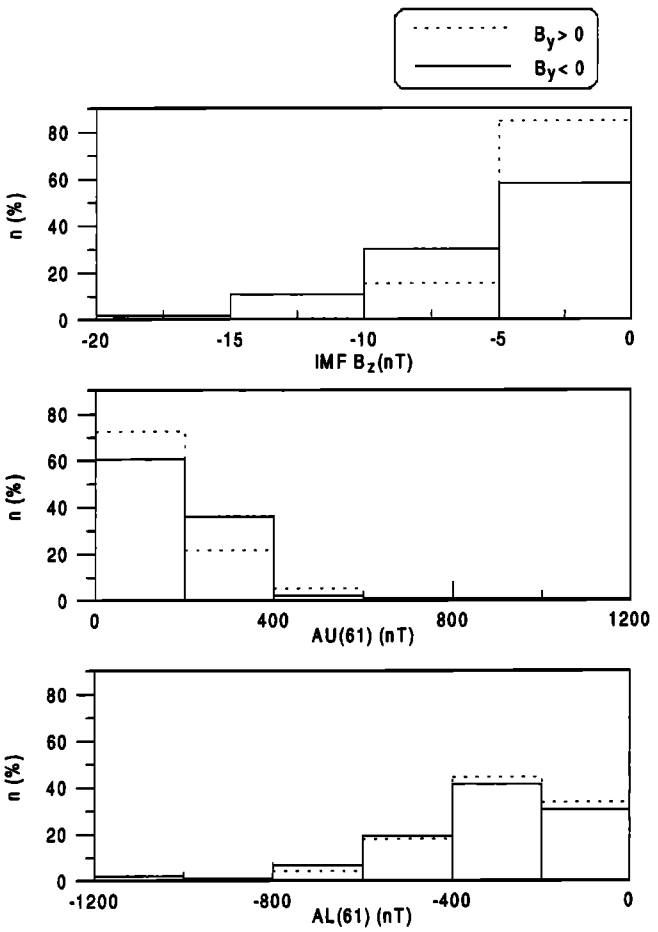

Figure 7. Histograms of IMF B_z, AU(61) and AL(61) shown separately for positive and negative IMF B_y during intervals of JH < 190 GW.

is rather sparse since the total number of magnetometric stations used for the Southern Hemisphere in our time interval is ~14% of the total number in the Northern Hemisphere, and there is only one Southern Hemisphere radar, at Halley Base, in comparison with the seven radars in the Northern Hemisphere. However, the JH(S) is presently the best estimation of JH(S) available, and the comparison in Table 2 could be in any case of some qualitative interest, with some warnings. In particular, the fact that the correlation coefficients of the polar cap geomagnetic activity with the JH(S) (shown in Table 2) are smaller than with the JH(N) (shown in Figure 4) can be attributed to the small data coverage in the Southern Hemsiphere.

However, one result of interest shown in Table 2 is related to the fact that, in effect, JH(S) is more directly related to AUS-80 than to ALS-80, and this effect is more important during the southward IMF, when substorm occurrence is associated with an increase of ionospheric conductance in the region of westward currents [*Vickrey et al.*, 1982; *Kamide et al.*, 1994]. This is in agreement with our results.

We note that we cannot find any level of JH(S) or IMF B_z above which the correlations in Table 2 break down similarly to the "saturation" found for JH(N). This might imply (with the warnings above about JH(S)) that this "saturation" is significantly affected by the hemispherical asymmeties [*Belon et al.*, 1969].

Moreover, Table 2 shows the occurrence of the best correlation between AES-80 and JH(S) during positive IMF B_z (coefficients 0.55 for positive B_y and 0.67 for negative B_y), which is in agreement with the expected polar shift of the auroral oval during northward IMF [*Kamide et al.*, 1976].

Finally, we note that during southward IMF the correlation coefficient shown in Table 2 between AUS-80 and JH(S) is higher during negative B_y than during positive. This is in agreement with the fact that a negative IMF B_z and B_y are associated with a higher contribution to JH(S) from eastward currents. Taking into account the model of interplanetary-magnetospheric interaction above, this means a smaller contribution to JH(N) of eastward current during negative IMF B_z and B_y [*Belehaki and Rostoker*, 1996], which is in agreement with our expectations.

4. Summary and Conclusions

We have compared the JH(N) with the AES-80 regional index for the southern polar cap. This comparison is significant in the context of previous findings about the possibility of using the PC index from Thule as a proxy of the JH(N), which implies an optimal cor-

Table 2. Correlation Coefficients of AES-80, ALS-80, and AUS-80 With JH(S) for Different Orientations of IMF B_y and B_z[a]

	$B_y > 0 - B_z > 0$ n=314	$B_y < 0 - B_z > 0$ n=265	$B_y > 0 - B_z < 0$ n=853	$B_y < 0 - B_z < 0$ n=261
AES-80	0.55	0.67	0.49	0.51
ALS-80	0.38	0.51	0.26	0.23
AUS-80	0.40	0.52	0.55	0.65

[a]Here n indicates the number of 5-min data points used in each correlation.

respondence of polar cap geomagnetic activity with the hemispherical JH production rate.

The period under study includes a very intense geomagnetic storm during the days October 18-23, 1995. During this interval the correlation between JH(N) and the southern polar index AES-80 is statistically significant at a confidence level above 99.9%, regardless of the hemispherical dependence of the observations.

The correspondence of AUS-80 to JH(N) is better than the one of ALS-80 to JH(N). This result has been interpreted in terms of the higher electric field characterizing the regions of eastward currents with respect to the regions of westward ones [e.g., *Vickrey et al.*, 1982].

The correspondence between JH(N) and the geomagnetic activity in the southern polar cap is better during periods of negative IMF B_y and B_z. Taking into account the above association of eastward currents and JH, our result is in agreement with the magnetospheric model that considers an increase of conductivity in the regions of eastward currents associated with negative IMF B_y and B_z in the Northern Hemisphere [*Belehaki and Rostoker*, 1996]. According to the same magnetospheric model, for negative IMF B_z, the contribution to JH(S) from regions associated with eastward currents is expected to be higher during negative than during positive B_y. In order to verify this, we calculated the best AMIE estimation of JH(S), and we found that for negative IMF B_z, the correlation between AUS-80 and JH(S) is higher during negative than during positive B_y. Therefore JH(S) results are in agreement with expectations too.

When the JH(N) is higher than 190 GW, the correspondence of southern polar cap geomagnetic activity and the JH(N) becomes null, in association with the occurrence of very high geomagnetic disturbances and of an IMF B_z component that exceeds -20 nT. This "saturation" effect is in part attributed to the shift of the auroral oval electrojets toward lower latitudes, more distant from the nominal polar cap. Moreover, it is in agreement with the expectation of a hemispherical asymmetric distortion of geomagnetic field lines due to solar wind pressure with respect to the Earth-dipole orientation [*Belon et al.*, 1969, and references therein].

We note that the agreement between JH estimated from AES-80, JH(N)*, and the JH(N) estimated by the AMIE procedure can be optimized (reaching correlation coefficient well above 0.9) by taking into account the previous considerations about geomagnetic activity and IMF orientation. This result might suggest the possible use of AES-80 as a Southern Hemisphere proxy for JH.

Acknowledgments. We thank C. G. Maclennan for valuable comments. The research at McMurdo and the Automatic Geophysical Observatories is supported in part by the Office of Polar Programs of the U.S. National Science Foundation.

Janet G. Luhmann thanks Barbara Emery and another referee for their assistance in evaluating this paper.

References

Akasofu, S.-I., Energy coupling between the solar wind and the magnetosphere, *Space Sci. Rev., 28*, 121, 1981.

Ballatore, P., and C.G. Maclennan, Significance of the high-latitude geomagnetic index AES-80: Comparison with the PC index, *Earth Planets Space, 51*, 425, 1999.

Ballatore, P., C.G. Maclennan, M.J. Engebretson, M. Candidi, J. Bitterly, C.-I. Meng, and G. Burns, A new southern high-latitude index, *Ann. Geophys., 16*, 1589, 1998a.

Ballatore, P., C.G. Maclennan, and M.J. Engebretson, A new geomagnetic index for Antarctic latitudes, in *Conference Proceedings,* vol.62, edited by M. Colacino et al., pp. 377-380, Soc. Ital. di Fis., Bologna, Italy, 1998b.

Baumjohann, W., and Y. Kamide, Hemispherical Joule heating and AE index, *J. Geophys. Res., 89*, 383, 1984.

Belehaki, A., and G. Rostoker, Relationship between the dayside auroral electrojets and the DPY current, *J. Geophys. Res., 101*, 2397, 1996.

Belon, A.E., J.E. Maggs, T.N. Davis, K.B. Mather, N.W. Glas, and G.F. Hughes, Conjugacy of visual auroras during magnetically quiet periods, *J. Geophys. Res., 74*, 1, 1969.

Chun, F.K., D.J. Knipp, M.G. McHarg, G. Lu, B.A. Emery, S.Vennerstrm, and O.A. Troshichev, Polar cap index as a proxy for hemispheric Joule heating, *Geophys. Res. Lett., 26*, 1101, 1999.

Codrescu, M.V., T.J. Fuller-Rowell, and J.C. Foster, On the importance of E-field variability for Joule heating in the high latitude thermosphere, *Geophys. Res. Lett., 22*, 2393, 1995.

Cooper, M.L., C.R. Clauer, B.A. Emery, A.D. Richmond, and J.D. Winningham, A storm time assimilative mapping of ionospheric electrodynamics analysis for the severe geomagnetic storm of November 8-9, 1991, *J. Geophys. Res., 100*, 19,329, 1995.

Friis-Christensen, E., and J. Wilhjelm, Polar cap currents for different directions of the IMF in the Y-Z plane, *J. Geophys. Res., 80*, 1248, 1975.

Kamide, Y., J.L. Burch, J.D. Winningham, and S.I. Akasofu, Dependence of the latitude of the cleft on the interplanetary magnetic field and substorm activity, *J. Geophys. Res., 81*, 698, 1976.

Kamide, Y., et al., Ground-based studies of ionospheric convection associated with substorm expansion, *J. Geophys. Res., 99*, 19,451, 1994.

Li, F., T.L. Killeen, A.G. Burns, W. Wang, Q. Wu, R. Roble, L.A. Frank, and J.B. Siywarth, Modeling of high-latitude thermosphere Joule heating at high spatial/temporal resolution (abstract), *Eos Trans. AGU, 79*(17), Spring Meet. Suppl., S32, 1998.

Lu, G., A.D. Richmond, B.A. Emery, and R.G. Roble, Magnetosphere-ionosphere-thermosphere coupling: Effects of neutral winds on energy transfer and field-aligned current, *J. Geophys. Res., 100*, 19643, 1995.

Maclennan, C.G., L.J. Lanzerotti, S.-I. Akasofu, S.-I. Zaitzev, P.J. Wilkinson, A. Wolfe, and V. Popov, Comparison of "electrojet" indices from the northern and southern hemispheres, *J. Geophys. Res., 96*, 267, 1991.

Mizera, P.F., D.J. Gorney, and D.S. Evans, On the conjugacy of the aurora: High and low latitudes, *Geophys. Res. Lett., 14*, 190, 1987.

Newell, P.T., and C.-I. Meng, Hemispherical asymmetry in cusp precipitation near solstices, *J. Geophys. Res., 93*, 2643, 1988.

Richmond, A.D., and Y. Kamide, Mapping electrodynamic features of the high-latitude ionosphere from localized observations: Technique, *J. Geophys. Res., 93*, 5741, 1988.

Richmond,A.D., et al., Global measures of ionospheric elec-

trodynamic activity inferred from combined incoherent scatter radar and ground magnetometer observations, *J. Geophys. Res., 95,* 1061, 1990.

Rosenberg, T.J., and J.H. Doolittle, Studying the polar ionosphere and magnetosphere with automatic geophysical observatories: The U.S. program in Antarctica, *Antarct. J. U.S., 29* (5), 347, 1992.

Saroso, S., M. Sugiura, T. Iyemori, T. Araki, and T. Kamei, Derivation of polar cap AE indices, *Proc. NIPR Symp. Upper Atmos. Phys., 5,* 35-45, 1992.

Troshichev, O. A., V. G. Andrezen, S. Vennerstrm, and E. Friis-Christensen, Magnetic activity in the polar cap - A new index, *Planet. Space Sci., 36,* 1095, 1988.

Vickrey, J. F., R. R. Vondrak, and S. J. Matthews, Energy deposition by precipitating particles and Joule dissipation in the auroral ionosphere,*J. Geophys. Res., 87,* 5184, 1982.

P. Ballatore, Laboratoire de Physique et Chimie de l'Environnement/CNRS, Avenue de la Recherche Scientifique, 45071 Orleans, France. (ballator@cnrs-orleans.fr)

D.J. Knipp, Department of Physics, U.S. Air Force Academy, Colorado Springs, CO 80840.

L.J. Lanzerotti, Bell Laboratories, Lucent Technologies, Mountain Avenue, Murray Hill, NJ 07974. (ljl@bell-labs.com)

G. Lu, NCAR, UCAR, Boulder, CO 80307. (ganglu@hao.ucar.edu)

(Received October 18, 1999; revised July 10, 2000; accepted July 10, 2000.)